

Short Note

N-(6-Chloro-3-nitropyridin-2-yl)-5-(1-methyl-1*H*-pyrazol-4-yl)isoquinolin-3-amine

Valentin Wydra ¹, Stefan Gerstenecker ¹, Dieter Schollmeyer ², Stanislav Andreev ^{1,3}, Teodor Dimitrov ^{1,3}, Ricardo Augusto Massarico Serafim ¹, Stefan Laufer ^{1,3,4}  and Matthias Gehringer ^{1,3,*} 

- ¹ Department of Pharmaceutical and Medicinal Chemistry, Institute of Pharmaceutical Sciences, Eberhard Karls Universität Tübingen, Auf der Morgenstelle 8, 72076 Tübingen, Germany; valentin.wydra@uni-tuebingen.de (V.W.); stefan.gerstenecker@uni-tuebingen.de (S.G.); stanislav.andreev@pharm.uni-tuebingen.de (S.A.); teodor.dimitrov@uni-tuebingen.de (T.D.); ricardo.serafim@mnf.uni-tuebingen.de (R.A.M.S.); stefan.laufer@uni-tuebingen.de (S.L.)
- ² Department of Chemistry, Johannes Gutenberg-Universität Mainz, Duesbergweg 10-14, 55128 Mainz, Germany; scholli@uni-mainz.de
- ³ Cluster of Excellence iFIT (EXC 2180) 'Image-Guided & Functionally Instructed Tumor Therapies', Eberhard Karls Universität Tübingen, 72076 Tübingen, Germany
- ⁴ Tübingen Center for Academic Drug Discovery, Auf der Morgenstelle 8, 72076 Tübingen, Germany
- * Correspondence: matthias.gehringer@uni-tuebingen.de; Tel.: +49-7071-29-74582

Abstract: Here we describe the synthesis of *N*-(6-chloro-3-nitropyridin-2-yl)-5-(1-methyl-1*H*-pyrazol-4-yl)isoquinolin-3-amine via a three-step procedure including a Buchwald–Hartwig arylation with benzophenone imine and a highly regioselective nucleophilic aromatic substitution. The title compound was analyzed by nuclear magnetic resonance spectroscopy (¹H, ¹³C, HSQC, HMBC, COSY, DEPT90 and NOESY), high resolution mass spectrometry (ESI-TOF-HRMS) and infrared spectroscopy (ATR-IR) and its structure was confirmed by single crystal X-ray diffraction. The inhibitory potency of the title compound was evaluated for selected kinases harboring a rare cysteine in the hinge region (MPS1, MAPKAPK2 and p70S6Kβ/S6K2).

Keywords: 3-nitropyridines; nucleophilic aromatic substitution; Buchwald–Hartwig arylation; protein kinase inhibitors; covalent inhibitors



Citation: Wydra, V.; Gerstenecker, S.; Schollmeyer, D.; Andreev, S.; Dimitrov, T.; Massarico Serafim, R.A.; Laufer, S.; Gehringer, M. *N*-(6-Chloro-3-nitropyridin-2-yl)-5-(1-methyl-1*H*-pyrazol-4-yl)isoquinolin-3-amine. *Molbank* **2021**, *2021*, M1181. <https://doi.org/10.3390/M1181>

Academic Editor: R. Alan Aitken
Received: 28 December 2020
Accepted: 14 January 2021
Published: 18 January 2021

Publisher's Note: MDPI stays neutral with regard to jurisdictional claims in published maps and institutional affiliations.



Copyright: © 2021 by the authors. Licensee MDPI, Basel, Switzerland. This article is an open access article distributed under the terms and conditions of the Creative Commons Attribution (CC BY) license (<https://creativecommons.org/licenses/by/4.0/>).

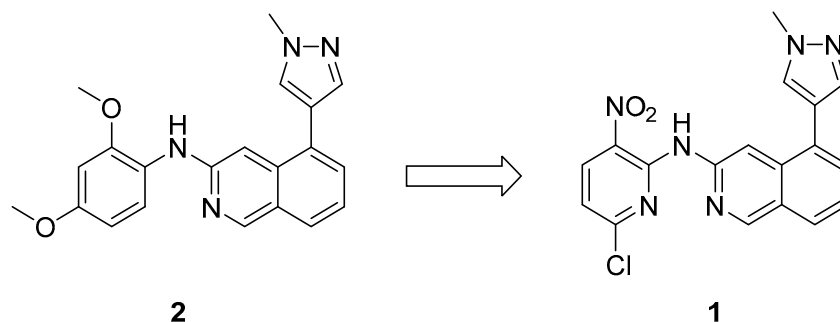
1. Introduction

The monopolar spindle 1 (MPS1) kinase, also known as threonine and tyrosine kinase (TTK) [1], is a potential therapeutic target for the treatment of various malignancies such as triple negative breast cancer [2]. The ongoing research on small molecules blocking MPS1 activity has led to the identification of potent inhibitors and even clinical candidates [3].

To address MPS1, we recently designed the potential irreversible inhibitor *N*-(6-chloro-3-nitropyridin-2-yl)-5-(1-methyl-1*H*-pyrazol-4-yl)isoquinolin-3-amine (**1**, Scheme 1). The structure was derived from *N*-(2,4-dimethoxyphenyl)-5-(1-methylpyrazol-4-yl)isoquinolin-3-amine (**2**), a potent reversible MPS1 inhibitor reported by Innocenti et al. [4]. The latter compound forms a crucial dual hydrogen bond between the 3-aminoisoquinoline core and the backbone of Gly605 located in the hinge region of the kinase [4].

Interestingly, the adjacent hinge residue in MPS1 is a poorly conserved cysteine (Cys604), which might be exploited in the development of selective targeted covalent inhibitors (TCIs) [5,6]. To address this rare cysteine, we sought to employ nucleophilic aromatic substitution (S_NAr) chemistry as a non-generic design approach [7]. Therefore, we combined the 5-(1-methyl-1*H*-pyrazol-4-yl)isoquinoline scaffold with an electrophilic 6-chloro-3-nitropyridine warhead (see compound **1**). This warhead type has been shown previously to engage a cysteine with an equivalent placement in the receptor tyrosine kinase FGFR4 [8]. As deduced from the latter study and our previous work on JAK3 inhibitors [9], the nitro group is not only required for activating the chloropyridine moiety for nucleophilic

aromatic displacement, but also to form a weak intramolecular hydrogen bond with the NH of the isoquinoline 3-amino group to promote the (re)active conformation.

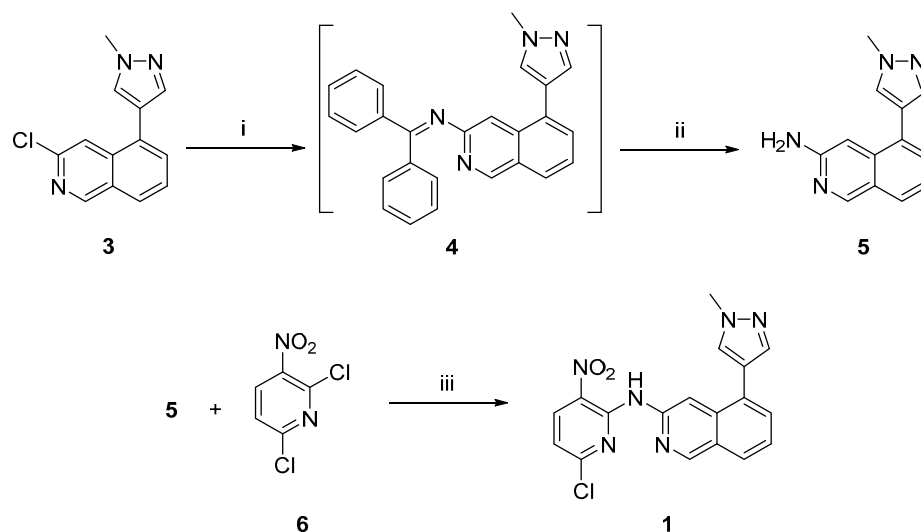


Scheme 1. Design of title compound **1** based on a 5-(1-methyl-1*H*-pyrazol-4-yl)isoquinoline scaffold.

2. Results and Discussion

2.1. Chemistry

The title compound **1** was prepared in three steps starting from previously reported 3-chloro-5-(1-methyl-1*H*-pyrazol-4-yl)isoquinoline (**3**) (Scheme 2) [4]. The amino group in the 3-position of the isoquinoline core was introduced following a modified protocol by Wolfe et al. [10]. To this end, **3** was subjected to a microwave-assisted Buchwald–Hartwig cross-coupling reaction with benzophenone imine generating intermediate **4**, which was subsequently hydrolyzed under acidic conditions. The resulting primary arylamine **5** was then reacted with commercially available 2,6-dichloro-3-nitropyridine (**6**) in the presence of *N,N*-diisopropylethylamine (DIEA) to furnish the title compound by regioselective nucleophilic aromatic substitution.



Scheme 2. (i) Benzophenone imine, Pd(OAc)₂, BINAP, *t*-BuONa, toluene, 130 °C (MW irradiation), 35 min; (ii) 2 N HCl_{aq.}, 75 °C, 1 h (77% over two steps); (iii) DIEA, 1,4-dioxane, reflux, 26 h (69%).

2.2. X-ray Crystallography

To demonstrate that the S_NAr reaction carried out in the final step of the synthetic route delivered the desired regioisomer, we determined the X-ray crystal structure of compound **1** (Figure 1). The data confirmed that nucleophilic substitution occurred in the 2-position of the 2,6-dichloro-3-nitropyridine precursor. The product shows the mentioned intramolecular hydrogen bond between the diarylamine NH and the nitro group. In addition, we observed two rotamers distinguished by the conformation of the methyl-substituted pyrazole ring.

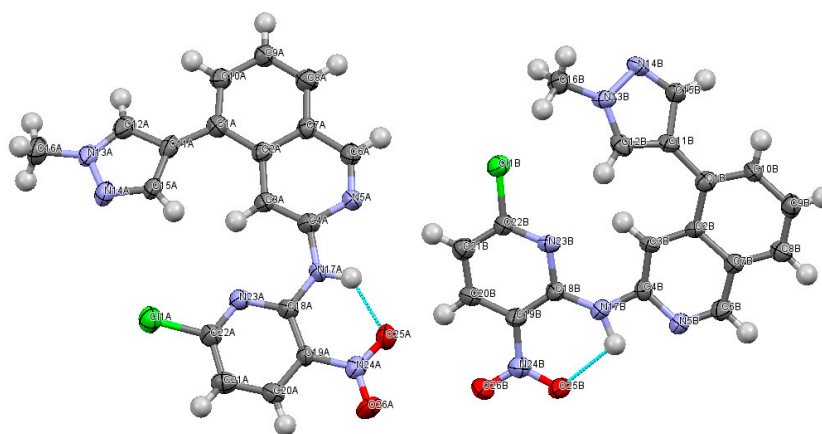


Figure 1. Structure of **1** determined by X-ray crystallography confirming the desired regiochemistry. The structure further demonstrates the formation of an intramolecular hydrogen bond between the nitro group and the diarylamine NH. Two rotamers were observed.

2.3. Biological Evaluation

The biological activity of compound **1** was evaluated in a radiometric HotSpot[®] kinase assay (Reaction Biology Corp. (Malvern, PA, USA)) [11] on selected kinases harboring the aforementioned cysteine in the middle hinge region (Table 1). While the compound did not show substantial activity on MAPKAPK2 and the intended target MPS1, it displayed an IC₅₀ value of 444 nM for the ribosomal s6 kinase p70S6Kβ (S6K2). As there are no selective p70S6Kβ inhibitors known so far, this compound may serve as a starting point for the design of such molecules.

Table 1. IC₅₀ values of compound **1** on selected kinases featuring a cysteine in the middle hinge region.

Kinase	IC ₅₀ [nM] ¹
MPS1	>5000
MAPKAPK2	>25,000
p70S6Kβ	444

¹ ATP concentration = 10 μM.

3. Materials and Methods

3.1. General Experimental Section

The utilized chemicals and reagents were of commercial quality and used without further purification, if not stated otherwise. Dry solvents were purchased from Fisher Scientific (Schwerte, Germany) and stored in septum-sealed bottles under N₂ atmosphere and over molecular sieves.

Purification via flash chromatography was performed on an Interchim PuriFlash 430 (Interchim, Montluçon, France) using Geduran Si 60–200 μm silica gel (Merck, Darmstadt, Germany) for pre-columns and Davisil LC60Å 20–45 μm silica gel (Grace Davison, Columbia, MD, USA) for preparative columns. The utilized mobile phases are described in the experimental procedures.

High-performance liquid chromatography (HPLC) was performed on an Agilent Technologies 1100 Series chromatographic system (Agilent Technologies, Santa Clara, CA, USA) equipped with an UV/Vis diode array detector (DAD) and a Phenomenex Luna[®] 5 μ (150 mm × 4.6 mm, 5 μm) reversed phase C8 separation column from Phenomenex (Phenomenex, Torrance, CA, USA). The mobile phase consisted of phase A (MeOH) and phase B (0.01 M KH₂PO₄-Buffer, pH = 2.3) and elution was performed at a flowrate of 1.5 mL/min using the gradient described in Table 2. The injection volume was 10 μL. The purity was determined at 254 nm and 230 nm.

Table 2. Mobile phase gradient applied in high-performance liquid chromatography.

	Time [min]		MeOH [%]			0.01 M KH ₂ PO ₄ -Buffer pH = 2.3 [%]			
	0	=>	8	40	=>	85	60	=>	15
	8	=>	13	85	=>	85	15	=>	15
	13	=>	14	85	=>	40	15	=>	60
	14	=>	16	40	=>	40	60	=>	60

Mass spectrometry was performed on an Advion expression[®] compact mass spectrometer (Advion, Ithaca, NY, USA) with an electrospray ionization (ESI) ion-source equipped with an Advion plate express TLC plate reader (Advion, Ithaca, NY, USA). High resolution mass spectrometry (HRMS) was performed on a Bruker maXis 4G (Bruker Daltonik, Bremen, Germany) ESI-TOF high resolution mass spectrometer.

Nuclear magnetic resonance (NMR) spectroscopy was performed on a Bruker Avance III HD 400 MHz NMR spectrometer (Bruker, Billerica, MA, USA). The ¹H and ¹³C NMR spectra were calibrated against the residual proton or ¹³C signals of the deuterated solvents. Signals are reported in parts per million (ppm) relative to tetramethylsilane ($\delta = 0$ ppm).

Melting points (Mp.) were measured on a Mettler Toledo MP70 melting point system (Mettler-Toledo, Columbus, OH, USA).

Attenuated total reflection infrared (ATR-IR) spectroscopy was performed on a ThermoFisher Scientific Nicolet 380 Fourier transformation (FT)-IR spectrometer (ThermoFisher Scientific, Waltham, MA, USA). Relevant bands are reported as wavenumbers in cm⁻¹.

X-ray diffraction was performed on a STOE IPDS 2T diffractometer with Cu-K α I μ S Microfocus as source of radiation (STOE & Cie. GmbH, Darmstadt, Germany).

The radiometric HotSpot[®] kinase assay [11] was carried out commercially at Reaction Biology Corp. (Malvern, PA, USA).

3.2. Synthetic Procedures

3.2.1. 5-(1-Methyl-1H-pyrazol-4-yl)isoquinolin-3-amine (5)

700 mg of 3-chloro-5-(1-methyl-1H-pyrazol-4-yl)isoquinoline [4] (2.87 mmol, 1 eq.), 64 mg of Pd(OAc)₂ (0.29 mmol, 0.1 eq.), 632 mg of BINAP (0.86 mmol, 0.3 eq.) and 830 mg of *t*-BuONa (8.62 mmol, 3 eq.) were suspended in 10 mL of dry toluene in a microwave tube [10]. The reaction mixture was degassed and purged with argon and 1.04 g of benzophenone imine (5.74 mmol, 2 eq.) was added. The mixture was stirred at rt and under argon atmosphere for 10 min and subsequently at 130 °C under microwave irradiation for 35 min (including 5 min ramp time). After cooling down to rt, the mixture was concentrated under vacuum, 25 mL of a 2 N HCl_{aq.} solution was added and stirring continued at 75 °C for 1 h. After the completion of imine hydrolysis, the suspension was extracted twice with 100 mL of DCM. The aqueous layer was then basified to a pH of 8 with 30% (*w/w*) NaOH_{aq.} and extracted three times with 100 mL of ethyl acetate (EtOAc). The combined EtOAc phases were dried over Na₂SO₄ and concentrated under vacuum. The resulting crude product was then purified via flash chromatography (SiO₂, EtOAc: MeOH, gradient elution from 0 to 8% MeOH). The solid obtained was triturated with HPLC grade pentane for further purification. The suspension was filtered, and the residue was dried under high vacuum to yield 493 mg (77%) of the desired product as a red-brown powder. Mp.: 156.9 °C; ¹H NMR (400 MHz, CDCl₃) δ 8.86 (s, 1H), 7.71 (d, *J* = 8.3 Hz, 1H), 7.69 (s, 1H), 7.55 (s, 1H), 7.43 (d, *J* = 6.4 Hz, 1H), 7.23 (t, 1H), 6.99 (s, 1H), 4.61 (bs, 2H), 3.98 (s, 3H); ¹³C NMR (101 MHz, CDCl₃) δ 155.1, 152.0, 139.3, 137.6, 130.9, 129.4, 127.9, 127.2, 124.1, 122.8, 120.4, 97.7, 39.24 (for the NMR spectra including 2D NMR experiments (HSQC), see Supplementary Figures S1–S3); ESI-MS: 225 *m/z* [M+H]⁺, 223 *m/z* [M–H][–] (for the mass spectrum, see Supplementary Figure S4); HPLC: *t*_r = 2.208 min, purity: 99.1% (254 nm), 99.4% (230 nm) (for the chromatogram see, Supplementary Figure S5).

3.2.2. *N*-(6-Chloro-3-nitropyridin-2-yl)-5-(1-methyl-1*H*-pyrazol-4-yl)isoquinolin-3-amine (**1**)

40 mg of 5-(1-methyl-1*H*-pyrazol-4-yl)isoquinolin-3-amine (0.18 mmol, 1 eq.) and 69 mg of 2,6-dichloro-3-nitropyridine (0.36 mmol, 2 eq.) were dissolved in 3 mL of dry 1,4-dioxane. Subsequently, 93 μ L of *N,N*-diisopropylethylamine (DIEA) (1.25 mmol, 7 eq.) were added to the stirring solution. The reaction mixture was then heated to reflux for 26 h. After cooling down to rt, the solvent was removed under vacuum. The resulting crude product was purified via flash column chromatography (SiO₂, hexane: EtOAc, gradient elution from 40 to 100% EtOAc). The obtained solid was triturated with HPLC grade pentane for further purification. The suspension was filtered, and the residue was dried under high vacuum to yield 47 mg (69%) of the desired product as a carmine-colored powder. Mp.: 191.9 °C (under decomposition); ¹H NMR (400 MHz, CDCl₃) δ 10.84 (s, 1H), 9.06 (s, 1H), 9.01 (s, 1H), 8.52 (d, *J* = 8.6 Hz, 1H), 7.89 (s, 1H), 7.88 (s, 1H), 7.86 (d, *J* = 8.5 Hz, 1H), 7.69 (d, *J* = 7.0 Hz, 1H), 7.52 (t, *J* = 7.6 Hz, 1H), 6.90 (d, *J* = 8.6 Hz, 1H), 4.05 (s, 3H); ¹³C NMR (101 MHz, CDCl₃) δ 155.6, 151.7, 147.9, 146.2, 139.4, 138.1, 135.9, 131.1, 130.3, 129.6, 128.1, 127.0, 126.8, 126.1, 119.9, 114.9, 107.5, 39.4 (for the NMR spectra including 2D NMR experiments (HSQC, COSY, HMBC, and NOESY), see Supplementary Figures S6–S12); HR-ESI-MS (calculated/found): 403.06807/403.06856 *m/z* [M+Na]⁺ (for the mass spectrum, see Supplementary Figure S13); HPLC: *t_r* = 9.050 min, purity: 98.2% (254 nm), 98.2% (230 nm) (for the chromatogram, see Supplementary Figure S14). ATR-IR: 3326, 1570, 1482, 1384, 1249, 850, 754, 708, 637, 533 (for the IR spectrum, see Supplementary Figure S15). Crystals for X-ray analysis were obtained by vapor diffusion of diethyl ether into a 10 mg/mL solution of compound **1** in chloroform (298 K, 1 atm). Crystal data for C₁₈H₁₃ClN₆O₂ (*M* = 380.79 g·mol⁻¹): monoclinic space group P2₁/*n*, *a* = 7.3911(8) Å, *b* = 23.1658(19) Å, *c* = 18.9367(19) Å, β = 92.580(8)°, *V* = 3239.1(5) Å³, *Z* = 8, *T* = 120 K, μ (CuK α) = 2.349 mm⁻¹, *D*_{calc} = 1.562 m·gm⁻³, 21465 reflections measured (3.82° ≤ θ ≤ 68.32°), 21465 unique (*R*_{sigma} = 0.1803) which were used in all calculations. CCDC 2051917 contains the supplementary crystallographic data for this paper.

4. Conclusions

In this study, we established a synthesis for *N*-(6-chloro-3-nitropyridin-2-yl)-5-(1-methyl-1*H*-pyrazol-4-yl)isoquinolin-3-amine (**1**). The synthesis started from known 3-chloroisoquinoline derivative **3**, which was converted into unprecedented isoquinoline-3-amine derivative **5** via Buchwald–Hartwig arylamination with benzophenone imine followed by acid-promoted hydrolysis of the imine intermediate. From compound **5**, the desired compound could be obtained via regioselective nucleophilic aromatic substitution with 2,6-dichloro-3-nitropyridine. Both **5** and **1** were fully characterized and the regiochemistry of **1** was confirmed by X-ray crystallography. Although inhibitor **1** did not show the expected inhibitory potency on the intended target kinase, MPS1, we found significant activity on the kinase p70S6K β , which features an equivalent cysteine. The compound may thus serve as a starting point for the development of p70S6K β inhibitors.

Supplementary Materials: The following data are available online: Figure S1: ¹H NMR spectrum of **5**; Figure S2: ¹³C NMR spectrum of **5**; Figure S3: HSQC spectrum of **5**; Figure S4: ESI-MS spectrum of **5**; Figure S5: HPLC chromatogram of **5**; Figure S6: ¹H NMR spectrum of **1**; Figure S7: ¹³C NMR spectrum of **1**; Figure S8: DEPT90 spectrum of **1**; Figure S9: HSQC spectrum of **1**; Figure S10: COSY spectrum of **1**; Figure S11: HMBC spectrum of **1**; Figure S12: NOESY spectrum of **1**; Figure S13: HR-ESI-MS spectrum of **1**; Figure S14: HPLC chromatogram of **1**; Figure S15: IR spectrum of **1**. The crystallographic data for compound **1** was deposited (CCDC 2051917) and is available free of charge at <http://www.ccdc.cam.ac.uk>.

Author Contributions: Conceptualization: M.G.; chemical synthesis: V.W. with support from S.G., T.D. and R.A.M.S.; X-ray crystallography: D.S.; data analysis: V.W., D.S., S.G., S.A., R.A.M.S., T.D. and M.G.; funding and infrastructure: M.G. and S.L.; manuscript writing—original draft preparation: V.W., S.G., S.A.; manuscript writing—review and editing, V.W., S.G., S.A., R.A.M.S., D.S., T.D., S.L. and M.G. All authors have read and agreed to the published version of the manuscript.

Funding: This work was supported by the Institutional Strategy of the University of Tübingen (ZUK 63, German Research Foundation), the RiSC Program of the State Ministry of Baden-Württemberg for Sciences, Research and Arts, the Max Buchner Research Foundation and the Postdoctoral Fellowship Program of the Baden-Württemberg Stiftung. Funding by the German Research Foundation (Deutsche Forschungsgemeinschaft, DFG) under Germany's Excellence Strategy-EXC 2180—390900677 is further acknowledged.

Data Availability Statement: The data from this study are available in this short note and in its supplementary material. Further supplementary crystal data are available at CCDC under the deposition number 2051917.

Conflicts of Interest: The authors declare no conflict of interest.

References

1. Mills, G.B.; Schmandt, R.; McGill, M.; Amendola, A.; Hill, M.; Jacobs, K.; May, C.; Rodricks, A.M.; Campbell, S.; Hogg, D. Expression of TTK, a novel human protein kinase, is associated with cell proliferation. *J. Biol. Chem.* **1992**, *267*, 16000–16006. [[CrossRef](#)]
2. Maire, V.; Baldeyron, C.; Richardson, M.; Tesson, B.; Vincent-Salomon, A.; Gravier, E.; Marty-Prouvost, B.; De Koning, L.; Rigai, G.; Dumont, A.; et al. TTK/hMPS1 is an attractive therapeutic target for triple-negative breast cancer. *PLoS ONE* **2013**, *8*, e63712. [[CrossRef](#)] [[PubMed](#)]
3. Schulze, V.K.; Klar, U.; Kosemund, D.; Wengner, A.M.; Siemeister, G.; Stöckigt, D.; Neuhaus, R.; Lienau, P.; Bader, B.; Prechtel, S.; et al. Treating cancer by spindle assembly checkpoint abrogation: Discovery of two clinical candidates, BAY 1161909 and BAY 1217389, targeting MPS1 kinase. *J. Med. Chem.* **2020**, *63*, 8025–8042. [[CrossRef](#)] [[PubMed](#)]
4. Innocenti, P.; Woodward, H.L.; Solanki, S.; Naud, S.; Westwood, I.M.; Cronin, N.; Hayes, A.; Roberts, J.; Henley, A.T.; Baker, R.; et al. Rapid discovery of Pyrido[3,4-d]pyrimidine inhibitors of monopolar spindle kinase 1 (MPS1) using a structure-based hybridization approach. *J. Med. Chem.* **2016**, *59*, 3671–3688. [[CrossRef](#)] [[PubMed](#)]
5. Chaikuad, A.; Koch, P.; Laufer, S.A.; Knapp, S. The cysteinome of protein kinases as a target in drug development. *Angew. Chem. Int. Ed. Engl.* **2018**, *57*, 4372–4385. [[CrossRef](#)] [[PubMed](#)]
6. Gehringer, M. Covalent kinase inhibitors: An overview. In *Topics in Medicinal Chemistry*; Springer: Berlin/Heidelberg, Germany, 2020; pp. 1–52. [[CrossRef](#)]
7. Gehringer, M.; Laufer, S.A. Emerging and re-emerging warheads for targeted covalent inhibitors: Applications in medicinal chemistry and chemical biology. *J. Med. Chem.* **2019**, *62*, 5673–5724. [[CrossRef](#)] [[PubMed](#)]
8. Fairhurst, R.A.; Knoepfel, T.; Leblanc, C.; Buschmann, N.; Gaul, C.; Blank, J.; Galuba, I.; Trappe, J.; Zou, C.; Voshol, J.; et al. Approaches to selective fibroblast growth factor receptor 4 inhibition through targeting the ATP-pocket middle-hinge region. *Medchemcomm* **2017**, *8*, 1604–1613. [[CrossRef](#)] [[PubMed](#)]
9. Gehringer, M.; Forster, M.; Pfaffenrot, E.; Bauer, S.M.; Laufer, S.A. Novel hinge-binding motifs for janus kinase 3 inhibitors: A comprehensive structure–activity relationship study on tofacitinib bioisosteres. *Chem. Med. Chem.* **2014**, *9*, 2516–2527. [[CrossRef](#)] [[PubMed](#)]
10. Wolfe, J.P.; Åhman, J.; Sadighi, J.P.; Singer, R.A.; Buchwald, S.L. An ammonia equivalent for the palladium-catalyzed amination of aryl halides and triflates. *Tetrahedron Lett.* **1997**, *38*, 6367–6370. [[CrossRef](#)]
11. Anastassiadis, T.; Deacon, S.W.; Devarajan, K.; Ma, H.; Peterson, J.R. Comprehensive assay of kinase catalytic activity reveals features of kinase inhibitor selectivity. *Nat. Biotechnol.* **2011**, *29*, 1039–1045. [[CrossRef](#)] [[PubMed](#)]